

Article

Algebraic Nexus of Fibonacci Forms and Two-Simplex Topology in Multicellular Morphogenesis

William E. Butler Hoyos ^{1,*} , Héctor Andrade Loarca ², Kristopher T. Kahle ¹, Ziv Williams ¹, Elizabeth G. Lamb ³, Julio Alcántara ⁴ , Thomas Bernard Kinane ⁵ and Luis J. Turcio Cuevas ⁶

¹ Neurosurgical Service, Massachusetts General Hospital, Boston, MA 02114, USA; kahle.kristopher@mgh.harvard.edu (K.T.K.); zwilliams@mgh.harvard.edu (Z.W.)

² Department of Mathematics, Ludwig Maximilian University of Munich, 80333 Munich, Germany; andrade@math.lmu.de

³ Massachusetts General Hospital for Children, Boston, MA 02114, USA; lambes52525@gmail.com

⁴ Center for Analysis and Social Mathematics, École des Hautes Études en Sciences Sociales, 75006 Paris, France; julio.alcantara@egs.edu

⁵ Pediatric Pulmonology, Massachusetts General Hospital, Boston, MA 02114, USA; kinane.bernard@mgh.harvard.edu

⁶ Departamento de Matemáticas, Universidad Nacional Autónoma de México, Coyoacán 04510, México; ljtc@ciencias.unam.mx

* Correspondence: wbutler@mgh.harvard.edu; Tel.: +1-617-726-3801

Abstract: Background: Fibonacci patterns and tubular forms both arose early in the phylogeny of multicellular organisms. Tubular forms offer the advantage of a regulated internal milieu, and Fibonacci forms may offer packing efficiencies. The underlying mechanisms behind the cellular genesis of Fibonacci and tubular forms remain unknown. Methods: In a multicellular organism, cells adhere to form a macrostructure and to coordinate further replication. We propose and prove simple theorems connecting cell replication and adhesion to Fibonacci forms and simplicial topology. Results: We identify some cellular and molecular properties whereby the contact inhibition of replication by adhered cells may approximate Fibonacci growth patterns. We further identify how a component $2 \rightarrow 3$ cellular multiplication step may generate a multicellular structure with some properties of a two-simplex. Tracking the homotopy of a two-simplex to a circle and to a tube, we identify some molecular and cellular growth properties consistent with the morphogenesis of tubes. We further find that circular and tubular cellular aggregates may be combinatorially favored in multicellular adhesion over flat shapes. Conclusions: We propose a correspondence between the cellular and molecular mechanisms that generate Fibonacci cell counts and those that enable tubular forms. This implies molecular and cellular arrangements that are candidates for experimental testing and may provide guidance for the synthetic biology of hollow morphologies.

Keywords: mitosis; Fibonacci; golden ratio; epigenomics; simplex topology; cell adhesion; organogenesis; morphogenesis



Citation: Butler Hoyos, W.E.; Andrade Loarca, H.; Kahle, K.T.; Williams, Z.; Lamb, E.G.; Alcántara, J.; Kinane, T.B.; Turcio Cuevas, L.J. Algebraic Nexus of Fibonacci Forms and Two-Simplex Topology in Multicellular Morphogenesis. *Symmetry* **2024**, *16*, 516. <https://doi.org/10.3390/sym16050516>

Academic Editors: Tidjani Negadi and Michel Planat

Received: 16 March 2024

Revised: 8 April 2024

Accepted: 15 April 2024

Published: 24 April 2024



Copyright: © 2024 by the authors. Licensee MDPI, Basel, Switzerland. This article is an open access article distributed under the terms and conditions of the Creative Commons Attribution (CC BY) license (<https://creativecommons.org/licenses/by/4.0/>).

1. Introduction

The Golden Ratio $(1 + \sqrt{5})/2 \approx 1.618$ was recognized at least as early as 500 BCE by Phidias, after whom the symbol Φ remains named [1]. Naturalists over the centuries have commented on its presence in plants, mollusks, and vertebrates, it has been depicted in the arts, and it has been the subject of teleological conjecture [2–4]. Multicellular organisms evolved from unicellular organisms in the Precambrian period 580 million years ago, and appear to have evolved on more than one occasion [5]. Fibonacci forms are found among these organisms [6], and are found among primitive plants such as algae [7]. Nevertheless, the molecular or cellular mechanisms for its presence in multicellular organisms remain unknown. It plays a role in plant phyllotaxis and perhaps in cellular packing, but a broader

adaptive value, if any, remains unknown [8–11]. We investigate Golden Ratio mathematics and its implications regarding the ontogeny of multicellular organisms.

The Golden Ratio is real-valued, while cell population counts are whole-numbered. The Fibonacci numbers are the particular whole numbers that obey the recurrence relation $\mathcal{F}_{n+1} = \mathcal{F}_n + \mathcal{F}_{n-1}$, with $\mathcal{F}_0 = 1$ and $\mathcal{F}_1 = 1$, giving the sequence 1, 1, 2, 3, ... Binet's formula offers a way to connect the Golden Ratio to the Fibonacci numbers,

$$\begin{aligned}\mathcal{F}_n &= \frac{1}{\sqrt{5}}(\Phi^n - (-1/\Phi)^n) \\ &= \frac{1}{\sqrt{5}}\left(\left(\frac{1+\sqrt{5}}{2}\right)^n - \left(\frac{1-\sqrt{5}}{2}\right)^n\right).\end{aligned}\quad (1)$$

Like the Golden Ratio, forms of the Fibonacci numbers appear in ancient culture [12,13].

In this paper, we shift the Fibonacci index by one, with $f_n = \mathcal{F}_{n+1}$. With $f_1 = 1$ and $f_2 = 2$, this gives the sequence (1, 2, 3, 5, 8, ...). Under this convention, if we start with one cell and assume the cell population grows with the Fibonacci numbers, then f_n gives the population cell count at the n^{th} generation. Furthermore, this convention offers a combinatorial interpretation of f_n , giving the number of ways that the number n can be composed as sums of 1 and 2 [14]. This is seen in Section 7.

Single-celled and multicellular organisms both perform replication. Some single-celled organisms exhibit adhesion. For example, the bacterium *Streptococcus pneumoniae* may adhere into pairs and chains, and *Staphylococcus aureus* may adhere into clusters. We hypothesize that multicellular organisms differ from single-celled organisms by having replication and adhesion be mutually regulated phenomena. An example in multicellular organisms is contact inhibition, where the adhesion between two cells yields the coordinated replication of only one of them [15]. The inter-regulation of adhesion and replication enables more extensive structures with cellular specialization amidst topological variations.

1.1. Replication

A cell in a multicellular organism has a cell cycle divided broadly into two intervals, interphase and mitosis, as shown in Figure 1. Interphase includes the time interval where a cell makes its specialized contribution to an organism and is where it makes preparatory changes so that it may divide. The proportions of time spent in interphase and mitosis vary greatly, but generally, a cell spends much more time in interphase.

The first phase in interphase is G_1 (G as in *gap*). In G_1 , a cell increases its supply of proteins and organelles (such as mitochondria, which catalyze the conversion of oxygen into energy), and it grows in size. It may transition to and from the non-growing phase G_0 .

Chromosomal DNA is replicated in the S interval of interphase. After DNA replication, each chromosome has a pair with an identical DNA sequence. G_2 is a growth phase after DNA replication.

Mitosis (M) is a brief interval in the cell cycle where the cell divides into two. It consists of a prophase, where the chromosomes become dense; a metaphase, where the chromosome pairs line up on the equatorial plane; an anaphase, where the chromosome pairs detach into sister chromatids; a telophase, where the sister chromatids move apart and form separate nuclei; and abscission, where the membranes cleave to form two progeny cells.

Cytokinesis is the interval of mitosis between anaphase and telophase when the sister chromatids segregate. They are pulled apart by mitotic spindles composed of tubulin. Cytokinesis provides the proper distribution of genetic material and cytoplasm between the two progeny cells. It involves the formation of a contractile ring, composed of actin and myosin filaments, at the equatorial plane of the dividing cell. The contractile ring is oriented perpendicular to the spindles. The contractile ring contracts, leading to the formation of a cleavage furrow and eventually to abscission, the detachment of the two progeny cells. The relationships between the contractile ring and the spindle at abscission can encode polarities in the mitotic progeny [16–20].

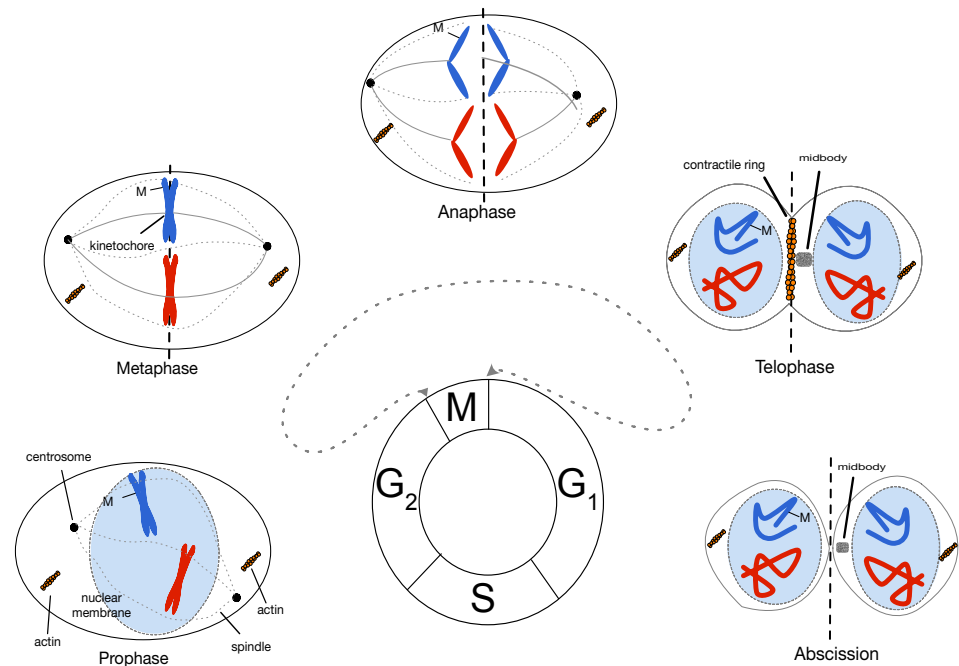


Figure 1. Cell cycle. Mitosis (*M*) occurs in a small fraction of the interval. The stages of mitosis are expanded. Some examples of potential differential epigenomics are shown. A methyl group (*M*) can be attached to a cytosine of a DNA strand prior to DNA replication. After replication, only one chromosome copy retains the methyl group. When spindles are helical, they can form enantiomeric relationships with chromosomal kinetochores upon chromosomal separation. A midbody positions itself along the contractile ring, which then may be inherited asymmetrically by one progeny cell upon abscission.

1.2. Adhesion

Adhesion is a persistent cell-to-cell connection with binding molecules that maintain the physical proximity between the adhered cells. It may occur by direct cell–cell contacts or be mediated by an intervening extracellular matrix. It may offer modes of communication or coordination between the cells.

There are broadly five types of molecular cell–cell adhesion types by direct contact, illustrated in Figure 2. A cell’s intracellular content is separated from the extracellular content by a bilipid membrane. In two of the adhesion types, gap junctions and tight junctions, lipid cell membranes between adjacent cells are intermingled. These adhesion types allow for the exchange of molecules between intracellular spaces. For the other three adhesion types, adherens junctions, desmosomes, and focal adhesions (with tunneling nanotubes), the adhesion is mediated by a multi-subunit protein structure that spans the extra- to the intracellular space [21]. The binding to the outer surface cell junctions generally induces metabolic changes within the cell. There is evidence that adhered cells can coordinate their cell cycles [22–24]. Furthermore, the tunneling nanotubes of focal adhesions enable intercellular exchange of DNA and RNA [21].

On the internal cell surface, the adhesion protein complex commonly binds to elements of the cytoskeleton. There are broadly three types of cytoskeleton protein. These are actin filaments, microtubules, and intermediate filaments such as vimentin [25]. Of these, actin filaments and microtubules are capable of active contraction. They play roles in modifying cell shapes and in cell migration. The cytoskeleton binds the inner surface of cell adhesion sites to intracellular organelles, including the cell nucleus. In mitosis, microtubules bind to chromosome pairs and pull them apart as a cell replicates. The cytoskeleton offers intracellular binding between the inner surface of cell adhesion sites [26].

The five types of cell–cell adhesions have differences in their properties, but the properties they have in common are that they physically bind adjacent cells together and may offer

signaling channels. This is the property of cell adhesion that we focus on, and we use adhesion as an umbrella term, but we do not treat the five cell–cell adhesion types separately. The extracellular matrix may offer indirect forms of cell-to-cell communication between cells not sharing a membrane for membrane adhesion. For example, molecules of the extracellular matrix may be anisotropic, and this anisotropy may be reflected intracellularly in the cellular cytoskeleton [27–29].

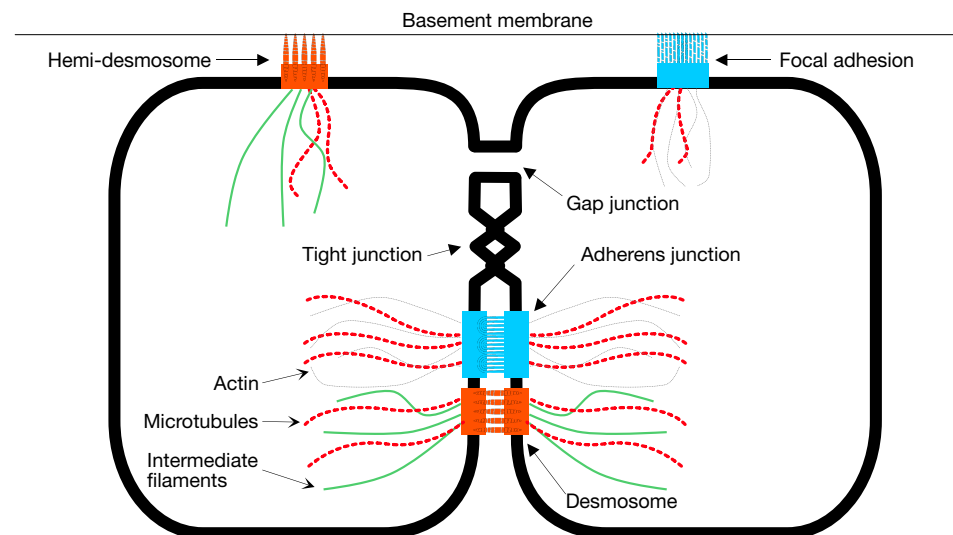


Figure 2. Adhesion types. The basement membrane is a form of extracellular matrix binding.

2. Cellular Adhesion and Replication Patterns That May Produce Fibonacci Population Counts

We identify patterns of cellular replication and adhesion that may produce Fibonacci population cell counts. For each of these, we ask what are the candidates for the underlying molecular apparatus. Then, we examine the properties of these cellular and molecular options for an adaptive advantage.

When we consider candidate molecular mechanisms behind Fibonacci cell kinetics, as per the central dogma of molecular biology [30], we assume that mitotic progeny share identical DNA sequences. Meiosis, not under consideration here, is a different type of cellular replication where, by design, the ultimate meiotic progeny have different chromosomes.

2.1. Differential Mitosis Timings between Progeny

Fibonacci (Leonardo Pisano) described a rabbit reproduction model based on two rabbit progeny with a different interval between birth and reproduction (Figure 3) [13]. The rabbit population grows with the Fibonacci numbers. We adapt this model to cell kinetics, substituting the replication unit of a rabbit pair with a cell in a multicellular organism. In this pattern, cells are assigned at birth to one of two cell cycle timing classes: r (replicate) and p (pause). Aside from cell cycle timing, the cells are of the same phenotype.

Analogous to Fibonacci’s rabbit reproduction model, at each generation, we model an r cell to replicate to another r cell plus a p cell. An r cell proceeds to mitosis while the p cell pauses for one generation then matures into an r cell that divides,

$$\begin{aligned} r &\mapsto r + p \\ p &\mapsto r \end{aligned} \quad (2)$$

We use subscripts to indicate the number of r and p cells in generation n ,

$$\begin{aligned} r_{n+1} &= r_n + p_n \\ p_{n+1} &= r_n. \end{aligned}$$

We express this in matrix notation as

$$\begin{pmatrix} r_{n+1} \\ p_{n+1} \end{pmatrix} = \begin{pmatrix} 1 & 1 \\ 1 & 0 \end{pmatrix} \begin{pmatrix} r_n \\ p_n \end{pmatrix}$$

where we recognize the Fibonacci Q matrix [31]

$$Q = \begin{pmatrix} 1 & 1 \\ 1 & 0 \end{pmatrix}.$$

The Q matrix can be used to generate the n^{th} Fibonacci number

$$\begin{pmatrix} f_n & f_{n-1} \\ f_{n-1} & f_{n-2} \end{pmatrix} = Q^n. \quad (3)$$

Furthermore, Golden Ratios appear in Q 's eigenvalues (Φ and $-1/\Phi$) [32]. Having Golden Ratio eigenvalues signifies that this model of divergent cell cycle timings can produce Φ generational sizes based on cells of two types of replication timings [33,34].

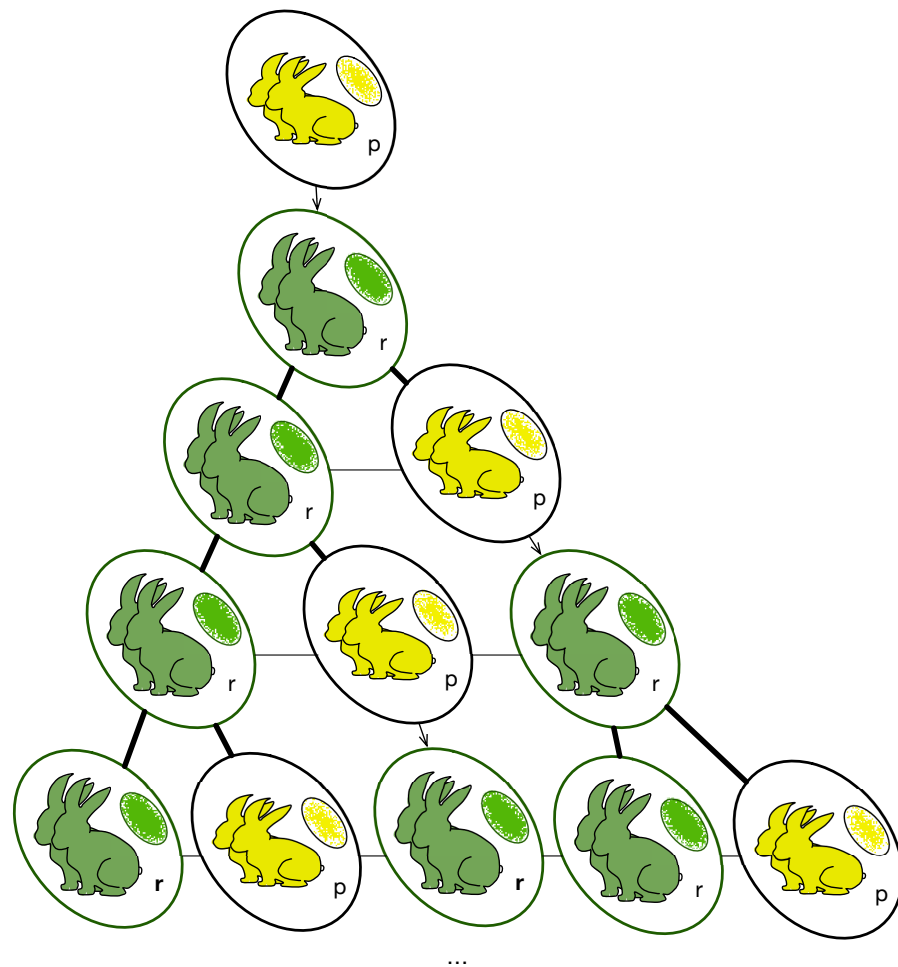


Figure 3. Fibonacci population growth in rabbits and cells with progeny with different lags after each reproduction. The thin horizontal lines represent adhesions.

This has similarities to the mathematics of L-systems as pioneered by Lindenmayer [35–37], and works on cellular automata [36,38–40].

Epigenomic Divergence

Epigenomics is the study of heritable changes in gene expression that do not rely on the primary DNA sequence [41]. Epigenomic phenomena participate in the regulation of cell metabolism, growth, and mitosis [42]. A differential mitosis timing between progeny could be accounted for if progeny were to diverge in their molecular epigenomics [43]. For example, there is an enzymatic apparatus that attaches methyl groups to the cytosine of DNA prior to replication in the *S* interval of interphase (Figure 1) [44]. This apparatus appears to have arisen early among eukaryotic cells, which are the foundation of multicellular organisms [45]. The methylated cytosine is not copied when a double strand of DNA is copied into two double strands in preparation for mitosis. Just one of the two progeny carries a particular cytosine methylation [46]. Insofar as this influencing mitosis timing, it might account for differential mitosis timings between progeny.

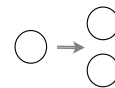
Histone methylation is another candidate mechanism for differential epigenomics [47,48]. The histone proteins help organize DNA strands into compact structures that can be contained in a cell nucleus. Histone methylation can influence the expression of genes in the associated DNA. Copies of histones are passed to mitotic progeny. This poses another opportunity for differential mitosis behavior between mitotic progeny.

There can be polarities in the mitotic progeny that derive from the relationship between the involuting spindle and the plane of the contractile ring at abscission [16–20].

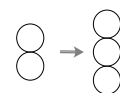
2.2. Contact Inhibition

In the model above, Fibonacci cell counts are generated by differential mitosis timings between progeny based on properties that are inhibited at cell birth. There is evidence though that cell cycles and mitosis timing can be coordinated by cell contacts [15]. We ask if there is a formalism to generate Fibonacci cell counts where cells that adhere coordinate to restrain mitosis in one of the two cells, whereas cells without contact (adhesion) mitose.

In one such pattern, adhered cell pairs coordinate their cell cycles so that only one undergoes mitosis. A single cell replicates to yield two cells



whereas with an adhered cell pair, one undergoes mitosis, producing three cells



This is contact inhibition [15].

Proposition 1. *There is an additive and recursive Fibonacci growth pattern based on contact inhibition. For illustration, we employ the language of biological cells.*

Proof. We demonstrate the existence of such an algorithm whereupon replication single cells go from count 1 to count 2 and cells pairs go from count 2 to count 3. The double arrow \Rightarrow denotes a replication step. We start with count 1.

$$f_1 \Rightarrow f_2$$

The two cells of f_2 coordinate to replicate into three cells. One cell comprising f_2 takes no replicative action. The other produces a copy of itself to give net

$$f_2 \Rightarrow f_3.$$

We proceed by induction for any $n \geq 3$. We start by rearranging

$$\begin{aligned} f_n &= f_{n-1} + f_{n-2} \\ &= (f_{n-2} + f_{n-3}) + f_{n-2} \end{aligned}$$

to give f_{n-2} pairs as

$$f_n = (f_{n-2} + f_{n-2}) + f_{n-3} \quad (4)$$

In the replication step, each pair coordinates to produce one more cell, $(f_{n-2} + f_{n-2}) \rightarrow 3f_{n-2}$ and each unpaired cell produces two, $f_{n-3} \rightarrow 2f_{n-3}$. This gives, upon replication,

$$\begin{aligned} f_n &\Rightarrow 3f_{n-2} + 2f_{n-3} \text{ (replication step)} \\ &= f_{n-2} + 2(f_{n-2} + f_{n-3}) \\ &= f_{n-2} + 2f_{n-1} \\ &= (f_{n-2} + f_{n-1}) + f_{n-1} \\ &= f_n + f_{n-1} \\ &= f_{n+1}. \end{aligned}$$

□

A given cell population may deviate from precise Fibonacci cell counts if, for example, in Equation (4), some of the cells enumerated by the f_{n-3} term form coordinated pairs, in which case they might form the epicenter of a new Fibonacci pattern, or if some cells in the f_{n-2} terms do not. A biological interpretation may be of variations in the local availability of cells to induce contact inhibition.

We introduce some terminology. In an adhered cell pair that undergoes replication, we term one cell the *partner cell* and the other the *mitosis cell*. There are two polarities that can be named. The orientation of the two cells relative to each other may be termed the *pair polarity*. With a mitosis cell, there is a *mitosis polarity*. This is given by the axis of sister chromatid separation. This corresponds to the axis from the centrosome at one pole of the cell to the centrosome at the other pole. The mitosis polarity is perpendicular to the plane defined by the contractile ring.

When two cells adhere, there may be a preference as to which is the partner cell and which is the mitosis cell. Furthermore, these preferences may have a relation to some directionality in the pair and mitosis polarities. Such a preference may be encoded intracellularly or in a difference in the relationship between the cell cytoskeleton and the extracellular matrix.

2.3. Cooperative Mitosis and Adhesion

In the above model of contact inhibition, when a pair of cells adhere, there is no preference as to which undergoes mitosis. However, recognizing the presence of epigenomic and polarity differences between mitotic progeny, there may be a biological circumstance where when two cells adhere; there is a molecular distinction between them that makes one in particular more apt to undergo mitosis. The biomolecular mechanisms behind such a distinction may transpire intracellularly or extracellularly, perhaps depending on polarities between a cell cytoskeleton and the extracellular matrix [49]. Let us assume that there are two cell types, a and b , that are similar in every way other than having a different preference to undergoing mitosis when they adhere.

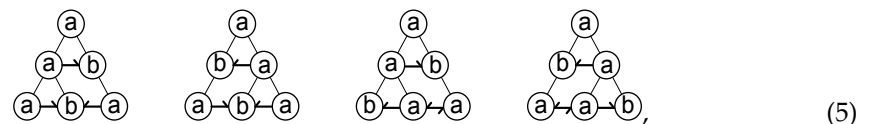
Proposition 2. *There is an additive and recursive Fibonacci growth pattern based on contact inhibition between cell types a and b . We denote this cell type by a left superscript. Replication from two cells to three is based on a pairing of an a cell with a b cell, $(a + b) \Rightarrow 2a + b$. An unpaired a cell replicates into an a cell and a b cell, $a \Rightarrow a + b$.*

Proof. Proceeding as above, and starting with n ,

$$\begin{aligned}
 f_n &= {}^a f_{n-1} + {}^b f_{n-2} \\
 &= ({}^a f_{n-2} + {}^b f_{n-2}) + {}^a f_{n-3} \\
 f_n &\Rightarrow (2{}^a f_{n-2} + {}^b f_{n-2}) + ({}^a f_{n-3} + {}^b f_{n-3}) \text{ (replication step)} \\
 &= (2{}^a f_{n-2} + {}^a f_{n-3}) + {}^b f_{n-2} + {}^b f_{n-3} \\
 &= {}^a f_{n-2} + {}^a f_{n-1} + {}^b f_{n-1} \\
 &= {}^a f_n + {}^b f_{n-1} \\
 &= f_{n+1}.
 \end{aligned}$$

□

A replication behavior that depends on and produces oriented adhesion between two cell types generates opportunities for emergent tissue patterns [49]. For example, using a half arrow head \rightarrow to denote an oriented adhesion between cells, we find that a number of tissue patterns may arise over three generations,



as indicated by the local orientations of cell types a and b .

A replication pattern based on cooperation between adhered cell pairs may approximate local Fibonacci growth for small n but it may not necessarily generate global Fibonacci patterns for large n .

3. Candidate Molecular Mechanisms

An assignment at adhesion to mitose or not is consistent with laboratory evidence that the five categories of cell adhesion (Figure 2) participate in gene and cell cycle regulation [50–55]. If these adhesion categories are able, in particular, to establish semaphore cell cycle coordination so that one of a pair undergoes mitosis, then Fibonacci population counts might be observed. If the paired cells are identical and the adhesion communication is symmetric, then it may be equal odds as to which cell of the adhered pair undergoes mitosis.

The molecular data are consistent with mutually reinforcing roles for mitosis and adhesion [15]. This might be the case if there is polarity among mitotic progeny that influences the mitosis semaphore at adhesion. The polarity-dependent mitotic behavior could span generations. A candidate molecular mechanism might be a cytoskeletal polarity that is linked across the cell membrane to polarities of extracellular adhesion and the extracellular matrix [27–29,56,57]. For example, the midbody, which forms along the cleavage line at telophase and can be asymmetrically inherited by a progeny [58], is involved in cell proliferation [59], and attaches to cell surface adhesion structures [54].

There are other opportunities for stereochemical variations between mitotic progeny with extracellular linkages. When chromosomes condense in the cell nucleus in the prophase, mitotic spindles form between centrosomes at opposite poles of the cell and attach to the kinetochores of the chromosomes (Figure 1). The spindles consist of microtubules which are motoric protein structures. They have a left chiral orientation as they link centrosome to centrosome at opposite cell poles. They attach to the kinetochores of chromosomes. Their chirality causes them to apply torque to chromosomes when they contract [60]. The helical spindle attachment to chromosomal kinetochores opens opportunities for stereoisomeric distinction upon chromosomal separation [61] (Figure 1). This opens an opportunity for enantiomeric chromosomal differences after the metaphase that remain coordinated with extracellular adhesion patterns.

4. Simplicial Steps by Replication and Adhesion

The sheer accumulation of mass by replication and adhesion may not be the most efficient way for a multicellular organism to gain an adaptive edge. There may be instead advantages from qualitative changes in shape. We ask how replication and adhesion, founded in molecular and cell biology, can enable the topological transformation of organism shape.

A topological transformation of bioontologic interest is the adoption of a tubular form. It enables a primitive organism to maintain a regulated internal environment with openings for exchanging nutrients and waste products with the external environment [49]. A hollow morphology that hosts a separated internal environment arose in some of the earliest multicellular organisms in the Precambrian period 580 million years ago, such as those from the phylum Cnidaria [62,63]. Fibonacci forms are found among these tubular plants and animals [6,7].

Another topological form of biological interest is the torus. It is a surface of revolution of a circle about a coplanar axis, reminiscent of a “donut” [64]. An internal torus form may offer a circulatory system. It may require a mechanical pump to impel cyclical fluid motion corresponding to a heart. There exist algorithms to construct three-dimensional objects such as a torus from two-simplex meshes [65]. A biological topic for investigation is whether there exist cellular and molecular mechanisms that might act like such algorithms to produce a torus. A torus provides greater control of the internal environment than a tube since the torus shape does not include a mouth-like opening. Instead, it relies on diffusion for chemical exchange with the environment. Among vertebrates, the circulatory system exchanges oxygen and carbon dioxide with the external environment by diffusion in the lungs.

We focus on the adoption by organisms of simple topological forms: the simplices. A topological k -simplex is a generalization of a directed multigraph with k vertices and a directed edge connecting every vertex pair, a face connecting every vertex triplet, and so on. A simplex reflects the most complex topological form representable by the fewest points. For a biological interpretation, we view cells as vertices and adhesions as edges, and we ask whether these roles might enable simplicial topological transformations. The study of simplices might offer insight into the genesis of complex biological forms from simpler ones by cellular replication and adhesion programs. A zero-simplex is a point, a one-simplex is two points with an edge between them, a two-simplex is a triangle with an outer boundary and a flat inner region, and so on.

In topology, there is an equivalence termed a homotopy between shapes that can be transformed into each other. If they can be continuously and invertibly transformed into each other, they are termed a homeomorphism. For example, the boundary of a two-simplex is the maximally continuously contracted form of a circle, and a circle is a continuously contracted form of a tube. Transitively, the boundary of a two-simplex is the maximally contracted form of a tube. We ask if there is an algebraic way to replicate the vertices of an n -simplex to produce an $n + 1$ -simplex. If so, we ask if there exists a cellular and molecular apparatus for executing this algebraic procedure to produce a biological two-simplex. If so, we further ask if there is a cellular and molecular apparatus for extending a biological two-simplex toward a circle of enlarging cellular diameter. A desired property of the cellular and molecular apparatus is that it enables a self-similar automaton program where individual cells act similarly in response to similar stimuli.

We define a simplex in terms of the barycentric coordinate system.

Definition 1 (n -Simplex). *Given $n + 1$ points v_0, v_1, \dots, v_n in R^n that are affinely independent, the n -simplex is the set of all points C_n*

$$C_n = \{ \lambda_0 v_0 + \lambda_1 v_1 + \dots + \lambda_n v_n \mid \sum_{i=0}^n \lambda_i = 1 \text{ and all } \lambda_i \geq 0 \}.$$

The affine dependence criterion assures that the simplex properties are preserved by an affine transform, which can include a linear scaling, a rotation, or a translation.

Definition 2 (Vertex Replication). *In an n -simplex with points C_n , the replication of the k^{th} point is given by a process:*

- Increase the space dimensions from R^n to R^{n+1} .
- This increases the vector length of every point. Let w_0, w_1, \dots, w_n be the first $n + 1$ points. Let each w_i be a copy of v_i with a zero placed in the last position.
- Let w_{n+1} be a copy of the point to be replicated, v_k , with a one placed in the last position.

Here is an example progression from a zero-simplex to a one-simplex to a two-simplex by two vertex replications.



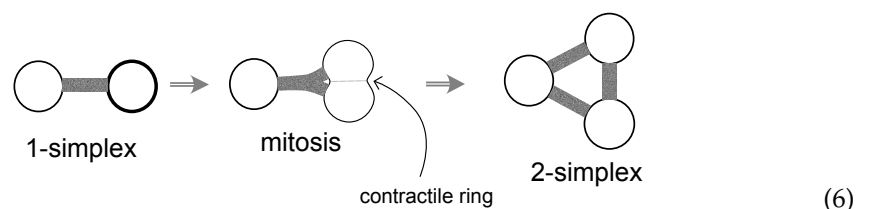
We find that a vertex replication in an n -simplex yields an $n + 1$ -simplex.

Theorem 1 (Simplex Growth by Vertex Replication). *A vertex replication in an n -simplex produces an $n + 1$ -simplex. The new simplex is given by the set of points*

$$C_{n+1} = \{ \lambda_0 v_0 + \lambda_1 v_1 + \dots + \lambda_{n+1} v_{n+1} \mid \sum_{i=0}^{n+1} \lambda_i = 1 \text{ and all } \lambda_i \geq 0 \}.$$

Proof. By assumption, prior to replication, the points v_0, v_1, \dots, v_n in R^n are affinely independent. It suffices to show that the produced points w_0, w_1, \dots, w_{n+1} in R^{n+1} are affinely independent. This holds because the point produced by replication, w_{n+1} , differs from all other points by having a one in its last vector position, whereas the $n + 1$ other points have a zero in that position. Therefore, w_{n+1} is affinely independent of all other points, which by assumption are affinely independent. □

In the contact inhibition model of Fibonacci cell count growth, an adhered cell pair assigns one as a partner cell and the other as a mitosis cell. Upon telophase, the mitosis cell forms a contractile ring. At cytokinesis, the contractile ring becomes the plane of abscission (Figure 1). We hypothesize that if the pair polarity is perpendicular to the mitosis polarity, then upon abscission, the polarity of the progeny cells will be perpendicular to the preceding pair polarity. This perpendicularity is equivalent to the affine independence of the progeny adhesion direction to the preceding pair polarity. In addition, if the mitosis polarity of the mitosing cell relative to the partner cell is such that their adhesion spans the contractile ring, then both progeny cells will inherit adhesion to the partner cell, in addition to retaining adhesion to each other, as shown in the first three steps here.

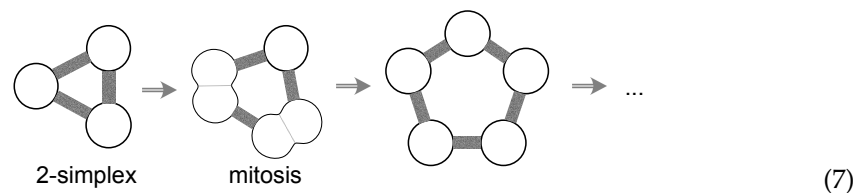


According to the simplex growth by vertex replication theorem, if the mitosis polarity is perpendicular to the pair polarity and if parental adhesions are inherited, then the original single cell produces a two-simplex at the third generation.

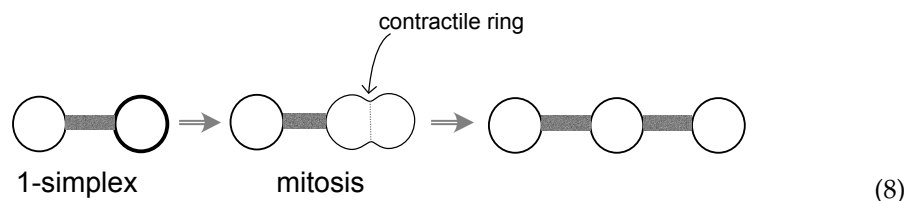
The capacity for a mitosing cell to split and share adhesions among progeny cells to a partner cell as in Equation (6) implies particular properties of cell membranes and

their embedded adhesion molecules. Rather than be an infinitesimally thin vertex between nodes as in graph theory, this implies an adhesion to be a bundle with a certain thickness that can be split. This appears to be consistent with the fluid mosaic biochemical theory, where “cell membranes are viewed as two-dimensional solutions of oriented globular proteins and lipids” [66]. Under this interpretation, the adhesion on the left-hand side of Equation (6) is formed by an arrangement of oriented proteins shared by segments of the liquid membranes of the two partner cells on the left. If the liquid zone of the dividing cell spans the plane of abscission, then both progeny cells inherit an adhered liquid zone on their cell membrane. If the two progeny cells retain adhesion by oriented proteins between them as their liquid membrane zones split across the plan of abscission, the resulting three cells will have the triangular shape of a two-simplex. These phenomena are consistent with the view of a cell membrane as a dynamic structure [67].

For mitoses starting with the fourth generation, the partner cell’s adhesion does not span the contractile ring or the plane of abscission. The restriction of the adhesion to one side of the plane of abscission allows the two-simplex to grow as a circle shape with every cell having a similar automaton program. The ensuing steps are not simplex progression because the orientations of the replication progeny are no longer affinely independent. After the two-simplex, the structure takes the form of a graph. An automaton program of self-similar replication and adhesion may be postulated for growth from a circle to a tube.



If the polarity of mitosis in the one-simplex relative to the partner cell is such that adhesion does not span the contractile ring, then a two-simplex will not form, as illustrated here.



A tubular morphology opens an opportunity for cellular specialization [49]. A two-layered cellular boundary that segregates an internal environment appears in some of the earliest multicellular organisms, such as those from the phylum Cnidaria [49,62,63,68]. The outer layer is termed the epidermis, and the inner layer the gastrodermis [63].

There is symmetry of the hole in the triangular form relative to the plane of the page on the right-hand side of Equation (6). This does not promote the morphogenesis of a directional body axis of a tubular organism. A directionality of the body axis is needed at morphogenesis to enable segmentation along the body axis and distinguish say, a mouth from an anus. Following the emergence of Cnidaria in the Precambrian era, a directional body axis facilitating segmentation arose with Ctenophora in the Cambrian era [69]. We identify a contact inhibition strategy between two cell types as capable of generating Fibonacci patterns. A directionality of a body axis could arise in turn from directionality in the adhesions of the cells that form the triangle of Equation (6) if the adhesion directions promote a right-hand chirality rule, but this is a topic for further research.

In vertebrates, tubular structures appear as the aero-digestive tract, the urinary tract, or endocrine/glandular secretion tracts—the hole in the two-simplex functions as a mouth for nutrient entry into a regulated internal environment. There are internal structures that

do not have a “mouth”, such as the circulatory system, the lymphatic system, and the cerebrospinal fluid system. These do not contract to a two-simplex.

With the classical power of two replication, two cells mitose simultaneously in the transition from the second to the third generation. The topological shape of the four-cell adhered product depends on each cell’s relation to the other’s contractile ring and abscission plane. If the mitotic polarity of each dividing cell is perpendicular to that of the other cell, and if each progeny retains adhesion to its sibling and inherits the adhesion of its parent, then the four-cell unit should take the shape of a tetrahedron. This shape is akin to a three-simplex, which is the simplest contraction of a sphere. It has an internal environment without an opening to exchange nutrients and waste products with the external environment. If neither cell’s adhesions span the other’s contractile ring, then the four-cell result should take the shape of a row, as in Equation (8).

5. A Visual Representation of Algebraic Topology of Replication and Adhesion

While Fibonacci replication with adhesion across three generations to produce a two-simplex offers the most direct path for an organism to form an internal environment, we wish to identify other paths toward hollow organs. For example, we may explore the more general ontogenic circumstance where asynchronously stem cells migrate into a vicinity, individually replicate, and then aggregate into cellular assemblies possibly containing topological holes.

We offer a visual representation for algebraically symbolizing the replication and adhesion status of cellular aggregations, while visually depicting the opportunities for topological transformations. Plural adhesion slots per cell may be depicted. An arrow symbol gives the adhesion direction. The arrowhead is the = symbol, and adhesions on the left-hand side match the right-hand side. Branches on either side of the arrowhead are interpreted as addition, +.

We select the arrowhead as the = symbol because the molecular apparatus of cellular adhesion and the extracellular matrix both appear to be anisotropic [27,70,71]. While this implies that cell adhesion slots are anisotropic, this assumption is unnecessary. The visual representation could be adjusted accordingly, such as by using double-headed arrows.

In the following examples, we treat cells as replicating in Fibonacci patterns, but this restriction is unnecessary with this visual representation. Let us assume that a progenitor cell replicates in generations with cell counts given by the Fibonacci numbers (1, 2, 3, 5, 8, ...). We assume that the two progeny cells of a replication adhere to each other. We refer to these as the horizontal cell adhesion slot for the convenience of representation on the printed page. We further assume that the individual cells in an aggregation may adhere to cells in another aggregation. We refer to these as the vertical cell adhesion slots for presentation on the printed page. We provide an over and under arrow notation to track adhesions between cells of different aggregations.

An epithelium is a common tissue pattern where there are adhesions between cell aggregations of different morphogenic lineages. An epithelium has one or more layers of cells, but generically, an epithelium has two adhered layers, each facing a distinct environment. In primitive organisms such as coral and other coelenterate members of Cnidaria, the outer layer termed the epidermis faces the external environment, and the inner layer, the gastrodermis, faces the environment within the tube [63]. In animals with a heart and a circulatory system, commonly, one layer faces blood in the circulatory system. This is the endothelium. The other layer contacts the environment that it bounds. With skin, this is the epidermis. In the lungs, two layers separate air in the alveolar sacs from blood in capillaries across a narrow gas diffusion barrier. In the intestine, two layers separate blood from alimentation in its stages of digestion, along with the microbiome. In the kidney, two layers separate blood from urine. In glandular structures, two layers separate blood from a secretory product. In portions of the liver, for example, this might be blood from bile. In the passages that follow, an epithelial layer is an exemplary aggregation of adhered cells.

A slice through an idealized two-layered epithelium is illustrated in Figure 4, where a layered aggregation of sizes f_2 and f_3 are adhered to one of size f_4 . In Figure 4, the cells have only one vertical receptor. Therefore, the assembly in Figure 4 cannot anneal with other Fibonacci-sized cell aggregations into larger structures.

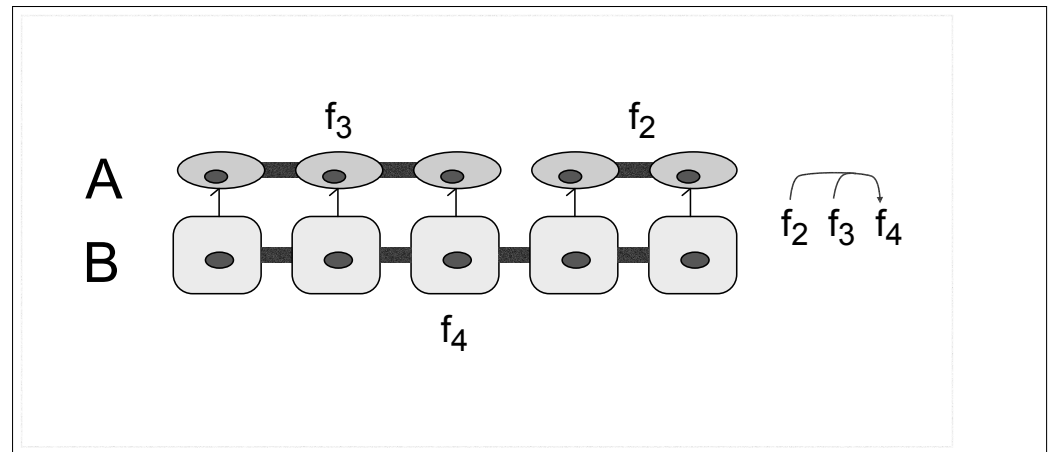


Figure 4. Single combinatorial engagement between three Fibonacci-sized cell aggregations. A two-layered epithelium (A) has concatenated cell aggregations of sizes $f_2 + f_3$ assembled onto a layer (B) of size f_4 by vertical one-to-one cell adhesion slots. Without dual adhesion by each cell, there is no chaining.

The function of the horizontal and vertical cell adhesion slots may be served by the same molecular pattern, but we segregate their visual representation above and below the cell count symbol because they serve different roles. The precise positions on a cell surface are not the focus of analysis. Instead, we are interested in the qualitative topological properties and are less interested in this analysis of morphological forms that can be deformed continuously into each other as topological homotopies.

In this notation, for example, we might represent $f_1 + f_2 = f_3$. These three assemblies may adhere across the = sign. We introduce an over/under arrow notation to indicate the top or bottom inter-aggregation adhesion sites. The arrowhead may be read as the equal = sign. For the top vertical slots, we may have, for example,

$$\overbrace{f_1 \ f_2 \ f_3} \quad (9)$$

This may represent the biological process whereby the top inter-aggregation cell adhesion slots of cell aggregations of sizes f_1 and f_2 adhere to and occupy the top adhesion slots of a cell aggregation of size f_3 . The vertical slots have sizes given by the Fibonacci number. This notation is specific to this application and is unrelated to the Fibonacci number of a graph [72]. This triplet is the simplest Fibonacci adhesion event involving cell aggregations of different sizes.

We exclude from consideration reflexive arrangements such as

$$\overbrace{f_5 \ f_5}$$

and

$$\overbrace{f_3 \ f_4 \ f_5}$$

that interrupt the chaining.

With this restriction, the presence of two vertical slots implies the potential for infinite chaining. For example, a set of Fibonacci-sized cell aggregations $f_1, f_2, f_3, f_4, f_5, f_6, \dots$ produced by kinetically tuned mitosis might assemble by overlapping triplet adhesion into a scaffold as

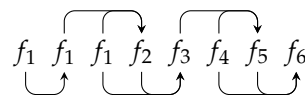


Such a structure may display a self-similar scaffold across the scales of size. Such a bio-fractal form may offer the biological efficiency of reuse of the same cell-to-cell adhesion molecules to maintain structural integrity across spatial scales. The same molecular apparatus that adheres one cell to another may adhere a lobule to a lobule, up to a limb to a trunk.

The Fibonacci numbers bring a rich set of combinatorial identities [73]. These combinatorial identities may be visually encoded to depict adhesion patterns between cells and cellular aggregations. For example, some Fibonacci identities produce a larger Fibonacci number from a collection of smaller ones. An example is

$$3f_1 + f_2 + f_3 + \dots + f_n = f_{n+2}.$$

If this represents a collection of Fibonacci-sized aggregations that adhere as



then as per the identity, the assembly would have f_8 cells. Accordingly, it may be contracted to the equivalent of a zero-simplex

$$f_8.$$

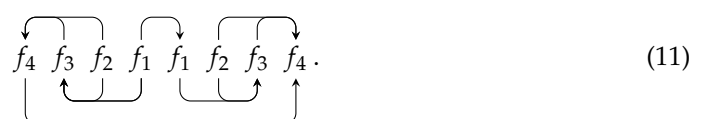
When Fibonacci-sized cellular aggregations combine, the resulting cell count is given by the theory of Fibonacci compositions [74].

6. Non-Simplicial Topological Transformation

Topological transformations may occur by the closure of discontinuities. Cellular aggregates that do not undergo topological transformations, such as into a two-simplex per Equation (6), may nonetheless combine and close discontinuities by adhesion. Two cellular aggregates may meet and adhere at two separate locations to jointly achieve a topological transformation. Alternately, a single cellular aggregate may fold so that formerly remote parts close by adhesion. The visual notation for representing adhesion among cellular aggregations allows us to explore circumstances where there may be topological transformations from adhesive closure of discontinuities.

When a collection of cellular aggregations finds an adhesion arrangement where all adhesion slots are occupied, we term this state full adhesion engagement. We assume that cells tend toward a fully engaged adhesion arrangement. We observe that an open scaffold such as in Equation (10) based on concatenated triplets cannot have full adhesion engagement because each terminus has one or more unoccupied adhesion slot.

However, if the two ends have unengaged vertical slots of equal size, then the structure can fold and bind into full engagement. An example is the palindrome



A palindrome is not the only closed form with full engagement. In Appendix A, we prove a set of conditions where a fully engaged ring can be made from random triplets of Fibonacci aggregations. With that proof in hand, we generate random numbers that conform to the terms of the proof to guarantee that the result will be a fully engaged scaffold ring (for example, see Figure 5).

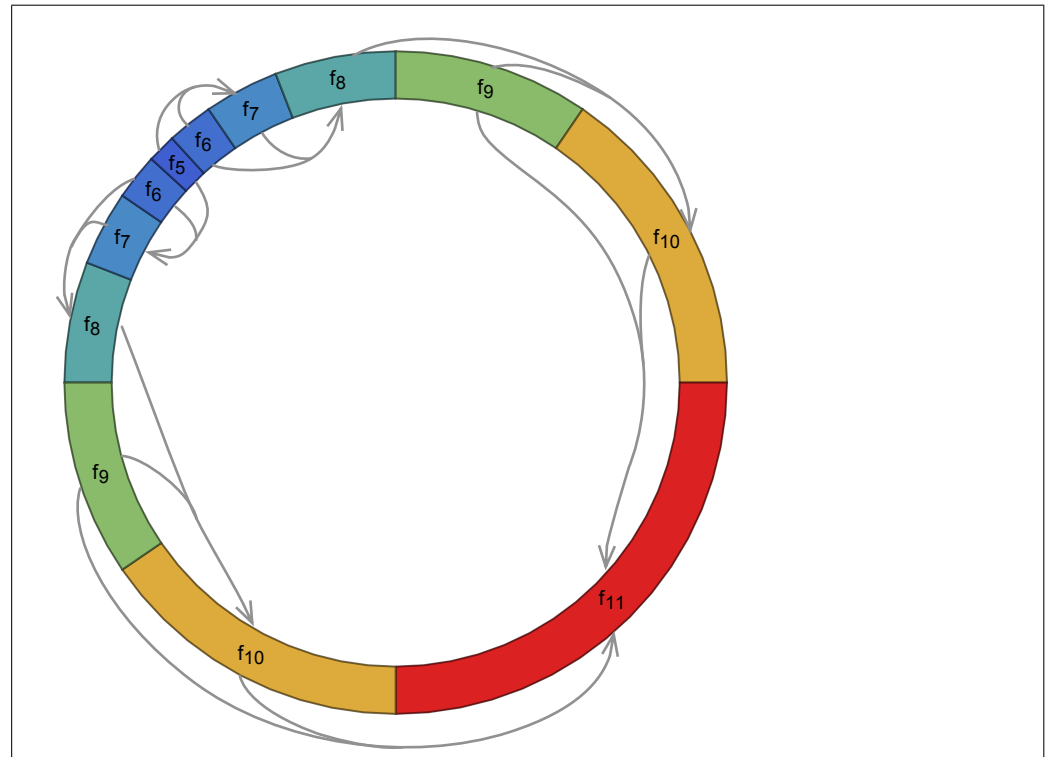


Figure 5. A scaffold ring. All inter and intra-aggregation adhesion slots are occupied. The arrows depict the inter-aggregation adhesion slot bindings.

7. Combinatorial Properties of Circular Forms

If several ring shapes of the same diameter were to stack up above and below the plane of the page and each cell were to have a further pair of unoccupied inter-aggregation adhesion slots oriented in the third dimension perpendicular to the plane of the page, then the rings could anneal into a tubular structure. We use the Fibonacci numbers to count the number of cells in a cellular aggregation, but the Fibonacci numbers offer a different combinatorial interpretation. For an open form of length n cell diameters, the Fibonacci number f_n carries the combinatorial interpretation of counting the number of ways to fill those n cell diameters with single cells and cell pairs. For a ring with a circumference of n cell diameters, that count is given by the Lucas number L_n [73] (p. 17 [75]). For a given number of cell diameters, the Lucas numbers are larger than the Fibonacci numbers, as per the identity

$$L_n = f_n + f_{n-2}$$

recalling that in our convention $\mathcal{F}_{n+1} = f_n$. This combinatorial relation is illustrated for a cellular two-simplex in Figure 6. As with the Fibonacci numbers, the ratio between adjacent Lucas numbers tends toward the Golden Ratio. Since the Lucas number is larger than the Fibonacci number for the same number of cells, a ring shape as a template offers a larger number of ways for single cells and pairs of cells to anneal to it than an open shape.

A circular assembly of cells appears to have greater entropy under a combinatorial Lucas tiling argument than an open assembly. This is further illustrated in Appendix A. If the same combinatorial forces act perpendicularly on the same cells, then a torus might

have greater entropy than a tube. Indeed, the topological square of a circle S^1 is a torus $S^1 \otimes S^1$. The shape resembles a circulatory system where pumped blood flows in circles. An idealized circulatory system with a two-chambered heart such as in gnathostome fish (Infraphylum Gnathostomata [76]) is illustrated in Figure 7.

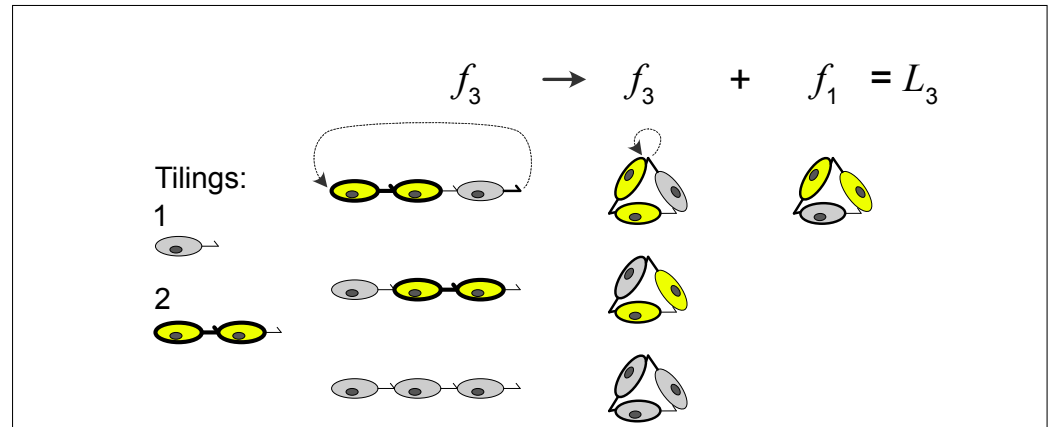


Figure 6. Cellular adhesion interpretation of the tilings heuristic for Fibonacci and Lucas numbers. There is a tiling of one cell (gray) and one of two cells (yellow). The number of tilings for a linear cell arrangement of length n is given by the n^{th} Fibonacci number $f_n = \mathcal{F}_{n-1}$. The number of tilings for a closed arrangement is given by the n^{th} Lucas number \mathcal{L}_n , where $\mathcal{L}_n = f_n + f_{n-2}$.

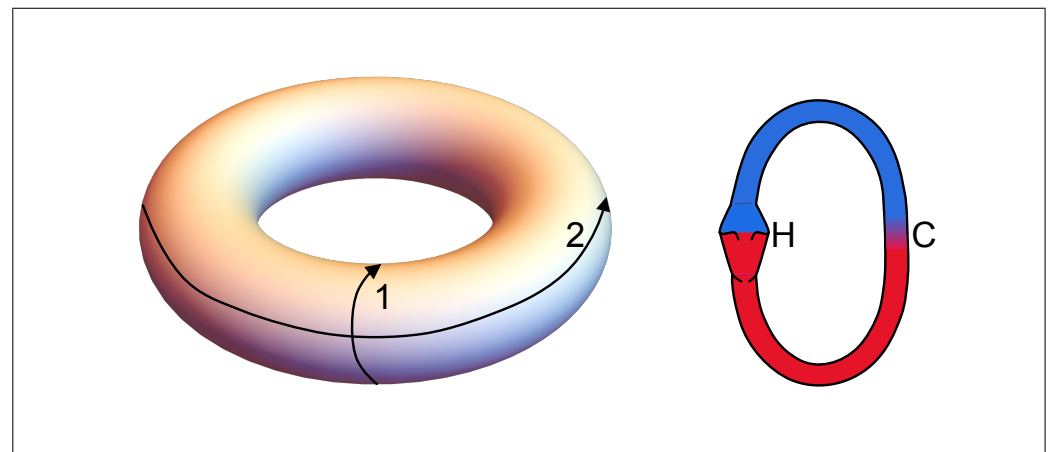


Figure 7. The topological square of a circular cellular aggregation (1) is a torus (2). This shares topological features with a primitive circulatory system shown here with an idealized two-chambered heart (H), an arterial component (red), a venous component (blue), and a capillary bed (C).

8. Conclusions

A multicellular organism is apt to gain adaptive advantages, not so much from sheer adhered mass, but by assuming topological forms not available to a unicellular organism. These topological forms can open survival strategies, such as a tubular form for hosting a regulated internal environment and providing a scaffold for cellular specialization. Under the terms of simplex topology, there is no simpler path by replication and adhesion for a multicellular organism to adopt a shape that is homotopic to a circle and a tube. An underlying molecular mechanism might be contact inhibition by adhered cells with particular polarities. Upon mitosis by one cell pair member, there is action across a fluid mosaic membrane to yield a cellular triplet in a two-simplex form. The identification of a laboratory model of tube formation might offer an experimental testbed for these predictions. An

alternate to such an analytic experimental strategy might be a synthetic strategy where notions such as these aid in a laboratory assembly of de novo tubular cellular forms [77].

This pathway depends on a contact inhibition model of replication. A pair of cells adhere to one another. By agreement, one undergoes mitosis, and the other does not. Under selected circumstances, this approximates Fibonacci growth patterns (Proposition 1). The progression to three adhered cells comprising a two-simplex depends on the adhered cells having a pair polarity perpendicular to a mitosis polarity and on the progeny cells inheriting the adhesions of the parent cell (Equation (6)). The “transition from individual replicators”, taken to be a common element among several major evolutionary steps [78–80], is favored in this analysis insofar as contact inhibition may favor replication and adhesion molecular patterns that can enable simplicial topological steps. A potentially advantageous example in multicellular organisms may be the adoption of tubular forms that can enable the maintenance of a comparatively stable internal milieu.

Author Contributions: Conceptualization, W.E.B.H., H.A.L., K.T.K., Z.W., E.G.L., J.A., T.B.K. and L.J.T.C.; methodology, W.E.B.H., H.A.L. and L.J.T.C.; formal analysis, W.E.B.H., H.A.L. and L.J.T.C.; resources, W.E.B.H.; writing—original draft preparation, W.E.B.H.; writing—review and editing, W.E.B.H., H.A.L., E.G.L. and L.J.T.C.; visualization, W.E.B.H.; supervision, W.E.B.H. and L.J.T.C.; project administration, W.E.B.H. and L.J.T.C. All authors have read and agreed to the published version of the manuscript.

Funding: This research received no external funding.

Data Availability Statement: Data are contained within the article.

Acknowledgments: Enrique Bojorquez critiqued the manuscript.

Conflicts of Interest: The authors declare no conflicts of interest.

Appendix A. Random Ring Patterns

To nourish our intuition, we wish to generate a family of random scaffold rings with full adhesion engagement. To start, we offer some definitions and provide a theorem showing that a scaffold ring as defined here has full adhesion engagement.

Definition A1. A Fibonacci triplet is a set of three aggregations of sequential Fibonacci size that have inter-aggregation receptor bindings to each other. A relative up triplet has increasing Fibonacci numbers such that a relative up triplet to f_{k-1} is

$$\begin{array}{c} \overbrace{\hspace{1.5cm}} \\ f_k \quad f_{k+1} \quad f_{k+2} \cdot \end{array}$$

and a relative down triplet is

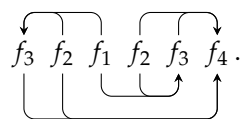
$$\begin{array}{c} \overbrace{\hspace{1.5cm}} \\ f_k \quad f_{k-1} \quad f_{k-2} \cdot \end{array}$$

It does not matter in this definition whether the inter-aggregation bindings are top or bottom.

Definition A2. A triplet scaffold is a structure that is composed of concatenated Fibonacci triplets where all slots are engaged and the summands and sums are contiguous.

We observe that in such a structure, a given triplet has six vertical adhesion slots. Two serve as summands to bind the concatenated triplet to the right. One serves as a sum to bind to two summands from the triple to the left. These overlapping Fibonacci relations bind the triplets one to the next in the scaffold. Three slots are internal to the triplet. Two of these are summands for a sum in a third slot.

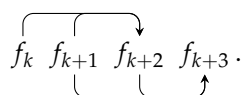
Definition A3. A scaffold ring is a triplet scaffold where the ends have folded to meet and adhere. An example is



Start with an arbitrary Fibonacci number, f_k , append to it an equal number of relative up and down triplets in arbitrary order, and adhere the slots.

Theorem A1. Such a ring has full adhesion engagement.

Proof. Start with an arbitrary initial Fibonacci number f_k . Append a relative up triplet. The rightmost aggregation is of size f_{k+3} because appending a triplet adds three to the rightmost Fibonacci index.



Append a relative down triplet. This subtracts three from the rightmost index.

$$f_k \quad f_{k+1} \quad f_{k+2} \quad f_{k+3} \quad f_{k+2} \quad f_{k+1} \quad f_k \quad (A1)$$

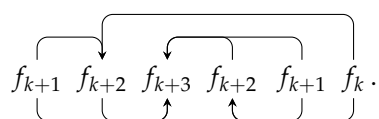
There are five internal Fibonacci-sized aggregations. These have 10 adhesion slots available. There are six sumand and four sum slots occupied, so the internal aggregations have full engagement. The aggregations on the left and right ends each have f_k occupied and f_k unoccupied slots. If the structure folds, the f_k -sized slots on each end will adhere because they are of the same size. Between the two triplets, we can insert an equal number of relative up and down triplets in random order and there will still be adhesion closure because each end will have f_k unoccupied vertical adhesion slots.

In the paragraph above, we start with a relative up triplet and end with a relative down triplet. We find, however, that the same argument holds whether we start or end with an up or down triplet so long as the number of them is equal. We also find that the order of the relative up and down triplets does not matter. □

Lemma A1. In a fully engaged ring, duplicating a Fibonacci-sized aggregation number or replacing a duplicate with a single produces a longer or shorter ring that still has full engagement.

This is because inserting a duplicate number only flips the vertical polarity of the ensuing receptor orientation. This lemma is nonsensical in the case of a palindromic ring where its successive application would cause the removal of all aggregations. Hybrid forms with an inner loop and open ends are algebraically possible but not treated here.

Removing the duplicate f_k from Equation (A1) produces



This is a triplet scaffold where the adhesions are fully engaged.

With this proof and lemma, we program a computer to generate some random scaffold rings with full engagement. We randomly generate a set of relative up and down triplets,

randomly insert and remove duplicates, and graph some results in Figure A1 to portray a range of allowed woven rings.

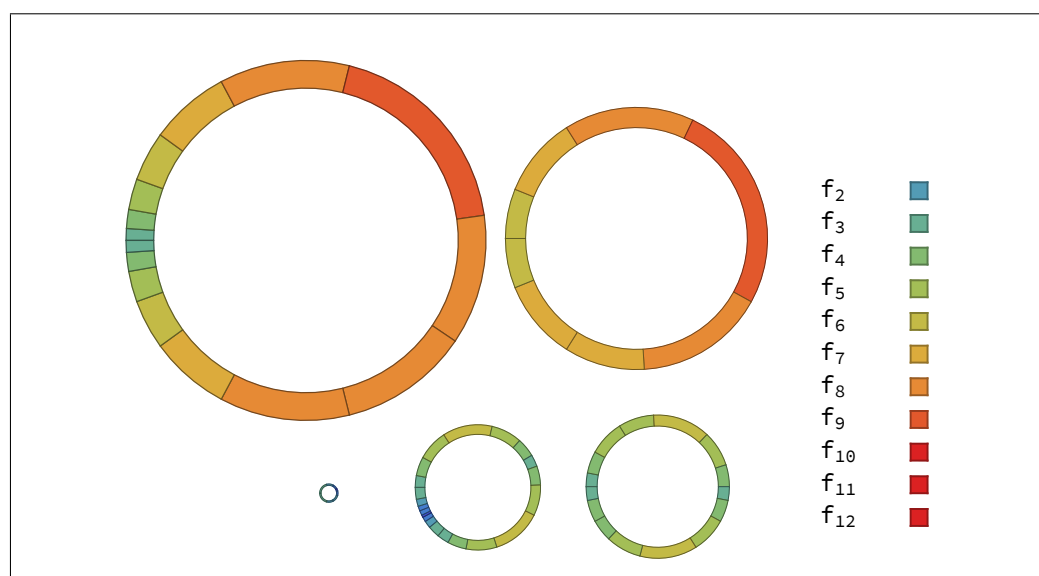


Figure A1. Some random woven rings. The legend gives the Fibonacci color code scheme. Cell binding relationships are not depicted.

References

1. Meisner, G.B. *The Golden Ratio*; Race Point Publishing: New York, NY, USA, 2018.
2. Livio, M. *The Golden Ratio*; Broadway Books: New York, NY, USA, 2008; p. 304.
3. de Campos, D.; Malysz, T.; Bonatto-Costa, J.A.; Pereira Jotz, G.; Pinto de Oliveira Junior, L.; Oxley da Rocha, A. Michelangelo, the Last Judgment fresco, Saint Bartholomew and the Golden Ratio. *Clin. Anat.* **2015**, *28*, 967–971. [[CrossRef](#)] [[PubMed](#)]
4. Iosa, M.; Morone, G.; Paolucci, S. Phi in physiology, psychology and biomechanics: The golden ratio between myth and science. *Biosystems* **2018**, *165*, 31–39. [[CrossRef](#)]
5. Sebé-Pedrós, A.; Degnan, B.; Ruiz-Trillo, I. The origin of Metazoa: A unicellular perspective. *Nat. Rev. Genet.* **2017**, *18*, 498–512. [[CrossRef](#)]
6. Wille, J.J. Occurrence of Fibonacci numbers in development and structure of animal forms: Phylogenetic observations and epigenetic significance. *Nat. Sci.* **2012**, *04*, 216–232. [[CrossRef](#)]
7. Peaucelle, A.; Couder, Y. Fibonacci spirals in a brown alga [*Sargassum muticum* (Yendo) Fensholt] and in a land plant [*Arabidopsis thaliana* (L.) Heynh.]: A case of morphogenetic convergence. *Acta Soc. Bot. Pol.* **2016**, *85*. [[CrossRef](#)]
8. Steurer, W.; Deloudi, S. Cluster packing from a higher dimensional perspective. *Struct. Chem.* **2011**, *23*, 1115–1120. [[CrossRef](#)]
9. Malygin, A.G. Morphodynamics of phyllotaxis. *Int. J. Dev. Biol.* **2006**, *50*, 277–287. [[CrossRef](#)] [[PubMed](#)]
10. Mughal, A.; Weaire, D. Phyllotaxis, disk packing, and Fibonacci numbers. *Phys. Rev. E* **2017**, *95*, 22401. [[CrossRef](#)] [[PubMed](#)]
11. Bozdag, G.O.; Zamani-Dahaj, S.A.; Kahn, P.C.; Day, T.C.; Tong, K.; Balwani, A.H.; Dyer, E.L.; Yunker, P.J.; Ratcliff, W.C. De novo evolution of macroscopic multicellularity. *bioRxiv* **2021**. [[CrossRef](#)]
12. Singh, P. The so-called fibonacci numbers in ancient and medieval India. *Hist. Math.* **1985**, *12*, 229–244. [[CrossRef](#)]
13. Sigler, L. *Fibonacci's Liber Abaci: A Translation into Modern English of Leonardo Pisano's Book of Calculation*; Springer Science and Business Media: New York, NY, USA, 2003.
14. Benjamin, A.T.; Plott, S.S. A combinatorial approach to fibonomial coefficients. *Fibonacci Q.* **2008**, *46-47*, 7–9.
15. Schnyder, S.; Molina, J.; Yamamoto, R. Control of cell colony growth by contact inhibition. *Sci. Rep.* **2020**, *10*, 6713. [[CrossRef](#)] [[PubMed](#)]
16. Lujan, P.; Rubio, T.; Varsano, G.; Köhn, M. Keep it on the edge: The post-mitotic midbody as a polarity signal unit. *Commun. Integr. Biol.* **2017**, *10*, e1338990. [[CrossRef](#)] [[PubMed](#)]
17. Juanes, M.; Piatti, S. The final cut: Cell polarity meets cytokinesis at the bud neck in *S. cerevisiae*. *Cell. Mol. Life Sci.* **2016**, *73*, 3115–3136. [[CrossRef](#)] [[PubMed](#)]
18. Johnson, A.; McCollum, D.; Gould, K. Polar opposites: Fine-tuning cytokinesis through SIN asymmetry. *Cytoskeleton* **2012**, *69*, 686–699. [[CrossRef](#)] [[PubMed](#)]
19. Fleming, E.; Zajac, M.; Moschenross, D.; Montrose, D.; Rosenberg, D.; Cowan, A.; Tirnauer, J. Planar spindle orientation and asymmetric cytokinesis in the mouse small intestine. *J. Histochem. Cytochem.* **2007**, *55*, 1173–1180. [[CrossRef](#)] [[PubMed](#)]

20. Caydasi, A.; Lohel, M.; Grünert, G.; Dittrich, P.; Pereira, G.; Ibrahim, B. A dynamical model of the spindle position checkpoint. *Mol. Syst. Biol.* **2012**, *8*, 582. [[CrossRef](#)] [[PubMed](#)]
21. Driscoll, J.; Gondaliya, P.; Patel, T. Tunneling Nanotube-Mediated Communication: A Mechanism of Intercellular Nucleic Acid Transfer. *Int. J. Mol. Sci.* **2022**, *23*, 5487. [[CrossRef](#)] [[PubMed](#)]
22. Gilberto, S.; Peter, M. Dynamic ubiquitin signaling in cell cycle regulation. *J. Cell Biol.* **2017**, *216*, 2259–2271. [[CrossRef](#)] [[PubMed](#)]
23. Ogura, Y.; Sasakura, Y. Emerging mechanisms regulating mitotic synchrony during animal embryogenesis. *Dev. Growth Differ.* **2017**, *59*, 565–579. [[CrossRef](#)]
24. Üretmen Kagali, Z.C.; Şentürk, A.; Özkan Küçük, N.E.; Qureshi, M.H.; Özlü, N. Proteomics in Cell Division. *Proteomics* **2017**, *17*, 1600100. [[CrossRef](#)] [[PubMed](#)]
25. Tang, D.; Gerlach, B. The roles and regulation of the actin cytoskeleton, intermediate filaments and microtubules in smooth muscle cell migration. *Respir. Res.* **2017**, *18*, 54. [[CrossRef](#)] [[PubMed](#)]
26. Rizzelli, F.; Malabarba, M.; Sigismund, S.; Mapelli, M. The crosstalk between microtubules, actin and membranes shapes cell division. *Open Biol.* **2020**, *10*, 190314. [[CrossRef](#)] [[PubMed](#)]
27. Dyson, R.J.; Green, J.E.F.; Whiteley, J.P.; Byrne, H.M. An investigation of the influence of extracellular matrix anisotropy and cell-matrix interactions on tissue architecture. *J. Math. Biol.* **2016**, *72*, 1775–1809. [[CrossRef](#)] [[PubMed](#)]
28. Motealleh, A.; Hermes, H.; Jose, J.; Kehr, N.S. Chirality-dependent cell adhesion and enrichment in Janus nanocomposite hydrogels. *Nanomed. Nanotechnol. Biol. Med.* **2018**, *14*, 247–256. [[CrossRef](#)] [[PubMed](#)]
29. Walma, D.A.; Yamada, K.M. The extracellular matrix in development. *Development* **2020**, *147*, dev175596. [[CrossRef](#)] [[PubMed](#)]
30. Ostrander, E.A. Central Dogma of Molecular Biology. 2022. Available online: <https://www.genome.gov/genetics-glossary/Central-Dogma> (accessed on 1 March 2024).
31. Gould, H.W. A history of the Fibonacci Q-matrix and a higher-dimensional problem. *Fibonacci Q.* **1981**, *19*, 250–257.
32. Silvester, J.R. Fibonacci Properties by Matrix Methods. *Math. Gaz.* **1979**, *63*, 188–191. [[CrossRef](#)]
33. Spears, C.; Bicknell-johnson, M.; Yan, J.J. Fibonacci phyllotaxis by asymmetric cell division: Zeckendorf and Wythoff trees. *Congr. Numer.* **2016**, *201*, 257–271.
34. Butler, W.; Kinane, T. Ring shape Golden Ratio multicellular structures are algebraically afforded by asymmetric mitosis and one to one cell adhesion. *bioRxiv* **2018**. [[CrossRef](#)]
35. Lindenmayer, A. Mathematical models for cellular interactions in development I. Filaments with one-sided inputs. *J. Theor. Biol.* **1968**, *18*, 280–299. [[CrossRef](#)] [[PubMed](#)]
36. Lindenmayer, A. Developmental algorithms for multicellular organisms: A survey of L-systems. *J. Theor. Biol.* **1975**, *54*, 3–22. [[CrossRef](#)] [[PubMed](#)]
37. Kelly-Sacks, C. The Biological and Mathematical Basis of L Systems. Ph.D. Thesis, Rochester Institute of Technology, Rochester, NY, USA, 1981.
38. Owens, N.; Stepney, S. Investigations of Game of Life cellular automata rules on Penrose Tilings: Lifetime and ash statistics. In Proceedings of the Automata 2008: Theory and Applications of Cellular Automata, Bristol, UK, 12–14 June 2008; pp. 1–35.
39. Giavitto, J.L.; Michel, O. Modeling the topological organization of cellular processes. *BioSystems* **2003**, *70*, 149–163. [[CrossRef](#)] [[PubMed](#)]
40. Nehaniv, C.L.; Rhodes, J.L. The evolution and understanding of hierarchical complexity in biology from an algebraic perspective. *Artif. Life* **2000**, *6*, 45–67. [[CrossRef](#)] [[PubMed](#)]
41. Kim, J.; Samaranyake, M.; Pradhan, S. Epigenetic mechanisms in mammals. *Cell. Mol. Life Sci.* **2009**, *66*, 596–612. [[CrossRef](#)]
42. Holliday, R. Epigenetics: A historical overview. *Epigenetics* **2006**, *1*, 76–80. [[CrossRef](#)] [[PubMed](#)]
43. Fuentealba, L.; Eivers, E.; Geissert, D.; Taelman, V.; De Robertis, E. Asymmetric mitosis: Unequal segregation of proteins destined for degradation. *Proc. Natl. Acad. Sci. USA* **2008**, *105*, 7732–7737. [[CrossRef](#)]
44. Charlton, J.; Downing, T.; Smith, Z.; Gu, H.; Clement, K.; Pop, R.; Akopian, V.; Klages, S.; Santos, D.; Tsankov, A.; et al. Global delay in nascent strand DNA methylation. *Nat. Struct. Mol. Biol.* **2018**, *25*, 327–332. [[CrossRef](#)]
45. Zemach, A.; McDaniel, I.E.; Silva, P.; Zilberman, D. Genome-wide evolutionary analysis of eukaryotic DNA methylation. *Science* **2010**, *328*, 916–919. [[CrossRef](#)]
46. Brero, A.; Leonhardt, H.; Cardoso, M.C. Replication and Translation of Epigenetic Information. In *DNA Methylation: Basic Mechanisms*; Springer: Berlin/Heidelberg, Germany, 2006.
47. Podobinska, M.; Szablowska-Gadomska, I.; Augustyniak, J.; Sandvig, I.; Sandvig, A.; Buzanska, L. Epigenetic Modulation of Stem Cells in Neurodevelopment: The Role of Methylation and Acetylation. *Front. Cell. Neurosci.* **2017**, *11*, 23. [[CrossRef](#)]
48. Laugesen, A.; Helin, K. Chromatin repressive complexes in stem cells, development, and cancer. *Cell Stem Cell* **2014**, *14*, 735–751. [[CrossRef](#)] [[PubMed](#)]
49. Dickinson, D.J.; Nelson, W.J.; Weis, W.I. An epithelial tissue in Dictyostelium challenges the traditional origin of metazoan multicellularity. *BioEssays* **2012**, *34*, 833–840. [[CrossRef](#)]
50. Yin, T.; Green, K. Regulation of desmosome assembly and adhesion. *Semin Cell Dev Biol* **2004**, *15*, 665–677. [[CrossRef](#)]
51. Díaz-Coránguez, M.; Liu, X.; Antonetti, D. Tight Junctions in Cell Proliferation. *Int. J. Mol. Sci.* **2019**, *20*, 5972. [[CrossRef](#)] [[PubMed](#)]
52. Balda, M.; Matter, K. Tight junctions and the regulation of gene expression. *Biochim. Biophys. Acta* **2009**, *1788*, 761–767. [[CrossRef](#)]
53. Le Bras, S.; Le Borgne, R. Epithelial cell division—Multiplying without losing touch. *J. Cell Sci.* **2014**, *127*, 5127–5137. [[CrossRef](#)]

54. Hatte, G.; Prigent, C.; Tassan, J. Adherens junctions are involved in polarized contractile ring formation in dividing epithelial cells of *Xenopus laevis* embryos. *Exp. Cell Res.* **2021**, *402*, 112525. [[CrossRef](#)]
55. Leithe, E. Regulation of connexins by the ubiquitin system: Implications for intercellular communication and cancer. *Biochim. Biophys. Acta* **2016**, *1865*, 133–146. [[CrossRef](#)]
56. Herszterg, S.; Pinheiro, D.; Bellaïche, Y. A multicellular view of cytokinesis in epithelial tissue. *Trends Cell Biol.* **2014**, *24*, 285–293. [[CrossRef](#)] [[PubMed](#)]
57. Dong, L.; Gong, J.; Wang, Y.; He, J.; You, D.; Zhou, Y.; Li, Q.; Liu, Y.; Cheng, K.; Qian, J.; et al. Chiral geometry regulates stem cell fate and activity. *Biomaterials* **2019**, *222*, 119456. [[CrossRef](#)]
58. Farmer, T.; Prekeris, R. New signaling kid on the block: The role of the postmitotic midbody in polarity, stemness, and proliferation. *Mol. Biol. Cell* **2022**, *33*, pe2. [[CrossRef](#)]
59. Peterman, E.; Prekeris, R. The postmitotic midbody: Regulating polarity, stemness, and proliferation. *J. Cell Biol.* **2019**, *218*, 3903–3911. [[CrossRef](#)] [[PubMed](#)]
60. Novak, M.; Polak, B.; Simunić, J.; Boban, Z.; Kuzmić, B.; Thomae, A.W.; Tolić, I.M.; Pavin, N. The mitotic spindle is chiral due to torques within microtubule bundles. *Nat. Commun.* **2018**, *9*, 3571. [[CrossRef](#)] [[PubMed](#)]
61. Satir, P. Chirality of the cytoskeleton in the origins of cellular asymmetry. *Philos. Trans. R. Soc. Lond. Ser. B Biol. Sci.* **2016**, *371*, 20150408. [[CrossRef](#)]
62. Schuchert, P. Phylogenetic analysis of the Cnidaria. *J. Zool. Syst. Evol. Res.* **2009**, *31*, 161–173. [[CrossRef](#)]
63. Berzins, I.K.; Yanong, R.P.E.; LaDouceur, E.E.; Peters, E.C. Cnidaria. In *Invertebrate Histology*; LaDouceur, E.E., Ed.; Wiley: Hoboken, NJ, USA, 2021; pp. 55–86.
64. Weisstein, E.W. From MathWorld—A Wolfram Web Resource. Available online: <https://mathworld.wolfram.com/Space.html> (accessed on 1 March 2024).
65. Flores, J.R.; de la Fraga, L.G. Basic three-dimensional objects constructed with simplex meshes. In Proceedings of the 1st International Conference on Electrical and Electronics (ICEEE), Acapulco, Mexico, 8–10 September 2004.
66. Singer, S.J.; Nicolson, G.L. The Fluid Mosaic Model of the Structure of Cell Membranes. *Science* **1972**, *175*, 720–731. [[CrossRef](#)]
67. Fletcher, A. The cell membrane and receptors. *Anaesth. Intensive Care Med.* **2007**, *8*, 443–446. [[CrossRef](#)]
68. Parfrey, L.W.; Lahr, D.J.G. Multicellularity arose several times in the evolution of eukaryotes (Response to DOI 10.1002/bies.201100187). *BioEssays* **2013**, *35*, 339–347. [[CrossRef](#)]
69. Pályi, G.; Zucchi, C.; Caglioti, L. Evolutionary origin of asymmetry in early metazoan animals. In *Advances in Biochirality*; Elsevier: Amsterdam, The Netherlands, 1999; p. 153.
70. Meng, W.; Takeichi, M. Adherens junction: Molecular architecture and regulation. *Cold Spring Harb. Perspect. Biol.* **2009**, *1*, a002899. [[CrossRef](#)]
71. Matsuzawa, K.; Himoto, T.; Mochizuki, Y.; Ikenouchi, J. alpha-Catenin Controls the Anisotropy of Force Distribution at Cell-Cell Junctions during Collective Cell Migration. *Cell Rep.* **2018**, *23*, 3447–3456. [[CrossRef](#)]
72. Knopfmacher, A.; Tichy, R.F.; Wagner, S.; Ziegler, V. Graphs, partitions and Fibonacci numbers. *Discret. Appl. Math.* **2007**, *155*, 1175–1187. [[CrossRef](#)]
73. Benjamin, A.; Quinn, J. *Proofs that Really Count*; The Mathematical Association of America: Washington, DC, USA, 2009.
74. Gessel, I.M.; Li, J. Compositions and Fibonacci Identities. *arXiv* **2013**, arXiv:1303.1366v3.
75. Koken, F.; Bozkurt, D. On Lucas numbers by the matrix method. *Hacet. J. Math. Stat.* **2010**, *39*, 471–475.
76. Stephenson, A.; Adams, J.W.; Vaccarezza, M. The vertebrate heart: An evolutionary perspective. *J. Anat.* **2017**, *231*, 787–797. [[CrossRef](#)] [[PubMed](#)]
77. Schwille, P. Jump-starting life? Fundamental aspects of synthetic biology. *J. Cell Biol.* **2015**, *210*, 687–690. [[CrossRef](#)]
78. Szathmáry, E.; Smith, J.M. The major evolutionary transitions. *Nature* **1995**, *374*, 227–232. [[CrossRef](#)]
79. Grosberg, R.K.; Strathmann, R.R. The Evolution of Multicellularity: A Minor Major Transition? *Annu. Rev. Ecol. Evol. Syst.* **2007**, *38*, 621–654. [[CrossRef](#)]
80. Fisher, R.M.; Cornwallis, C.K.; West, S.A. Group formation, relatedness, and the evolution of multicellularity. *Current Biol.* **2013**, *23*, 1120–1125. [[CrossRef](#)]

Disclaimer/Publisher’s Note: The statements, opinions and data contained in all publications are solely those of the individual author(s) and contributor(s) and not of MDPI and/or the editor(s). MDPI and/or the editor(s) disclaim responsibility for any injury to people or property resulting from any ideas, methods, instructions or products referred to in the content.